Josephson effect in superconductor/ferromagnet-normal/superconductor structures

T. Yu. Karminskaya,[1,*] A. A. Golubov,[2] M. Yu. Kupriyanov,[1] and A. S. Sidorenko[3]
[1]*Nuclear Physics Institute, Moscow State University, 119992 Moscow, Russia*
[2]*Faculty of Science and Technology and MESA+ Institute of Nanotechnology, University of Twente, P.O. Box 217, 7500 AE Enschede, The Netherlands*
[3]*Institute of Electronic Engineering and Industrial Technologies ASM, Chisinau MD2028, Moldova*
(Received 22 December 2008; revised manuscript received 13 May 2009; published 9 June 2009)

The critical current I_C of superconductor/ferromagnet-normal/superconductor (S/FN/S) Josephson junctions is calculated in the framework of linearized Usadel equations. The dependence of I_C on the distance L between superconductors and thicknesses $d_{F,N}$ of ferromagnetic and normal layers is analyzed. It is shown that $I_C(L,d_F)$ may exhibit damping oscillations as a function of both arguments. The conditions have been determined under which the decay length and period of oscillation of $I_C(L)$ at fixed d_F are on the order of decay length of superconducting correlations in the N metal, ξ_N, that is much larger than in F film. We demonstrate also that the positions of the points $L=L_n$, at which $I_C=0$ exhibit damping oscillations as a function of d_F. The number of transitions from 0 to π states in $I_C(L,d_F)$ increases under $L\to L_n$. Outside these narrow intervals of L around L_n sign and value of I_C are independent on d_F for $d_F \gtrsim \xi_F$. This fact is important for possible applications of S/FN/S Josephson junctions and S/FNF/S spin valve Josephson devices.

DOI: 10.1103/PhysRevB.79.214509 PACS number(s): 74.45.+c, 74.50.+r, 74.78.Fk, 75.30.Et

I. INTRODUCTION

In the last few years there have been considerable efforts on searching ferromagnetic materials suitable for fabrication of superconductor (S)/ferromagnetic (F)/superconductor (S) Josephson junctions for small-scale applications.[1–19] The analysis of existing experimental data[16,17] have shown that the value of exchange energy H in ferromagnetic materials used in[1–19] scales is in between 850 and 2300 K. This leads to effective decay length $\xi_{F1}\approx 1.2–4.6$ nm and period of oscillations $\xi_{F2}\approx 0.3–2$ nm of thickness dependence of a S/F/S junction critical current I_C. These values turned out to be much smaller compared to the decay length $\xi_N \approx 10–100$ nm, in similar S/normal metal (N)/S structures. This fact makes it difficult to fabricate S/F/S junctions with reproducible parameters. It also leads to suppression of I_CR_N product (where R_N is the normal-state resistance of the junction), thus limiting the cutoff frequency of the junctions. Since a search of exotic ferromagnetic materials with smaller value of H is a challenging problem,[20] one has to seek for another solutions.

A possible way to increase the decay length in a ferromagnetic barrier is the use of long-range proximity effect due to induced spin-triplet superconductivity[21–40] in structures with nonuniform magnetization. A recent survey of possible structures in which the long-range proximity effect may exists can be found in Refs. 39 and 40. If magnetization of a ferromagnetic barrier is homogeneous, then only singlet component and triplet component with projection $S_z=0$ of the total Cooper-pair spin are induced in the F region (see Refs. 22 and 23). These superconducting correlations are short ranged, i.e., they extend into the F layer over a short distance on the order of $\xi_{F1}=\sqrt{D_F/H}$ in the diffusive case (here D_F is the electronic diffusion coefficient of F). However, in the case of inhomogeneous magnetization, e.g., in the presence of magnetic domain walls or in SF multilayer with noncollinear directions of magnetization of different F layers, a long-range triplet component with $S_z=\pm 1$ may appear. Since this triplet component is an even function of the momentum, it must be an odd function of the frequency and, therefore, it is called the odd triplet component. It decays into F region over a distance $\xi_F=\sqrt{D_F/2\pi T_C}$ (here T_C is the critical temperature of S layer), which is by the factor $\sqrt{H/2\pi T_c}$ larger than ξ_{F1}. The latter property might lead to the long-range effects observed in some experiments.[41,42]

The transformation of decay length from ξ_{F1} to ξ_F might also take place in a vicinity of a domain wall even without generation of an odd triplet component.[43–51] This enhancement depends on an effective exchange field which is determined by thicknesses and exchange fields of the neighboring domains. If a sharp domain wall is parallel[47,50] or perpendicular to SF interface[51] and the thickness of ferromagnetic layers, $d_f \lesssim \xi_{F1}$, then for antiparallel direction of magnetization the exchange field effectively averages out, and the decay length of superconducting correlations becomes close to that of a single nonmagnetic N metal $\xi_F=\sqrt{D_F/2\pi T_C}$. It should be mentioned that for typical ferromagnetic materials ξ_F is still small compared to decay length $\xi_N \gtrsim 100$ nm of high-conductivity metals such as Au, Cu, or Ag. This difference can be understood if one takes into account at least two factors. The first one is that typical values of Fermi velocities in ferromagnetic materials (see, e.g., the analysis of experimental data done in Refs. 16 and 17) are on the order of 2×10^5 m/s, which is about 1 order of magnitude smaller than in high-conductivity metals. The second factor is rather small electron mean-free path in ferromagnets, especially in alloys such as CuNi, PtNi, etc.

Another possible solution of the problem of enhancement of the decay length is based on the effect of suppression of H due to the proximity effect between ferromagnetic and normal metal films.[52–54] In such junctions a weak link region consists of FN or FNF multilayer which separates the superconducting banks, while a supercurrent flows in the direction parallel to FN interfaces. There are two kinds of proximity

effects in these structures. The first one is the penetration of superconductivity into normal metal from superconducting electrodes. The second one is the suppression of the induced superconductivity due to interaction between N and F layers. It is obvious that for nontransparent NF interfaces the S/FNF/S junction should have the same characteristics as that of SNS devices and the decay length of superconductivity into the complex weak link region should coincide with ξ_N if the distance between superconducting electrodes $L \gg \xi_{F1}$. In Refs. 52–54 it was shown that switching on interaction between N and F metals results in generation of a set of decay lengths. Moreover, it was demonstrated that it is possible to find the conditions under which at least one among of these lengths has both real and imaginary parts that scale in the range of ξ_N.

In S/FNF/S Josephson junctions it is also possible to solve another challenging problem. Namely, it is possible to realize a control upon the junction parameters by changing the mutual orientation of magnetization vectors of ferromagnetic films.

The idea of possibility of such a control has been intensively discussed earlier in S/F/S junctions having different complexities of weal link region. The first suggestions were concentrated on a tunnel S/F-dielectric (I)-F/S Josephson junctions which consist of S/F sandwiches separated by I layer.[24,55–59] It was shown that switching from parallel to antiparallel direction of F layer magnetization vectors may result in enhancement of critical current of these devices as well as in transition from π to zero states. However, it seems that practical realization of this switching is a rather complex task, which is difficult to implement. The next class of SFS junctions exploits the idea of interplay between singlet and odd triplet superconducting components inside a Josephson structure.[25–29] In SFSF devices,[25,26] where one of the F films is screened from the external magnetic field by a superconducting electrode, a change in direction of the upper F layer magnetization can be easier realized than in junctions having two or more F layers between superconducting banks. Unfortunately, to implement the effective I_C modulation it is necessary to fit two alternative conditions. On one hand, thickness of S layer in FSF part of the structure must be large enough in order to have a reasonable critical temperature. On the other hand, to provide the connectedness of the magnetization directions of the F films, which is necessary condition for generation of odd triplet component, this thickness must be small. The same problems occur in realization of FSF spin valve devices (see e.g. Ref. 60). In S/FNF/S Josephson junctions there is FNF control element that has several sharp distinctions from the discussed above structures having FSF or FIF control unit. The superconducting correlations induced into N layer exit due to proximity effect with S electrodes rather than to its own superconductivity. Consequently the limitation on the thickness of N layer is not too strong and it can be small enough to provide the necessary interaction between F layers. The next distinction is that for generation of the odd triplet component it is enough slightly (on the angle $\alpha \lesssim 10°$) deflect the direction of magnetization of one of F layers from initial antiferromagnetic configuration of F films magnetization vectors. It is also necessary to point out that in this domain of α decay the lengths of both

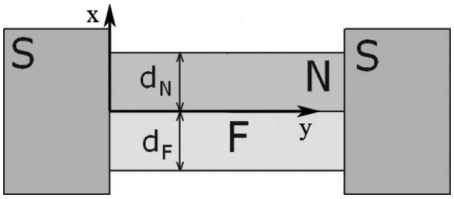

FIG. 1. Schematic view of the S/NF/S junction.

singlet and odd triplet superconducting components are real, they decay on ξ_N scale without any oscillations, and odd triplet superconducting components falls down more slowly compare to singlet one. At a given distance between superconducting electrodes $L \gtrsim \xi_N$ the last fact leads to transition of S/FNF/S spin valve from 0 to π state with α increase and it was demonstrated that the magnitude of I_C in this π state can be essentially larger than that for ferromagnetic configuration of magnetization. Recently the possibility of experimental realization of deflection of the magnetization direction of one of F layers from initial antiferromagnetic configuration of F films has been demonstrated in spin valve structure designed to control the critical temperature of superconducting film.[60]

The results obtained in Refs. 52–54 are essentially based on the assumption that the thicknesses d_N and d_F of all the films in FNF multilayer are small compared to their decay lengths. This assumption allows one to simplify the problem and to reduce two-dimensional problem to one dimensional.

In real structures the requirement $d_N \ll \xi_N$ can be easily fulfilled, while the inequality $d_F \ll \xi_F$ is difficult to achieve due to the smallness of ξ_F and finite roughness of NF interfaces. Therefore the solution of two-dimensional problem is needed. The structures with two-dimensional geometry were examined in Ref. 51 for two-domain junction, in Ref. 35 for multidomain SF structures, and in Ref. 37 for junction with helicoidal spin modulation.

It is worth to note that the solution of two-dimensional problem arising in the "in-plane" geometry, when the domain wall is perpendicular to SF interface,[46,51] is simplified by a natural for this problem suggestion that domain walls consist of materials differing only by the direction of their magnetization.

In this paper we will concentrate on properties of a generic S/FN/S junction and perform the calculation of its critical current beyond the limits of small F and N film thicknesses for two-dimensional geometry. Contrary to Refs. 46 and 51 in our approach we shall consider that NF interface has finite transparency and that N and F metals have different transport parameters. Under these conditions, the solution of the two-dimensional problem should be found, which is essentially more complicated compared to that discussed in Refs. 46 and 51.

II. JUNCTION MODEL

Consider a symmetric multilayered structure, which consists of a superconducting electrode contacting the end wall of a bilayer. This bilayer consists of F film and N having thicknesses d_F and d_N, respectively (see Fig. 1). We will

suppose also that the condition of a dirty limit is fulfilled for all metals and that effective electron-phonon coupling constant is zero in F and N films. For simplicity we suggest below that the parameters γ_{BN} and γ_{BF} which characterize the transparency of NS and FS interfaces,

$$\gamma_{BN} = R_{B1}\mathcal{A}_{B1}/\rho_N\xi_N, \quad \gamma_{BF} = R_{B2}\mathcal{A}_{B2}/\rho_F\xi_F,$$

are large enough,

$$\gamma_{BN} \gg \max\left\{1, \frac{\rho_S\xi_S}{\rho_N\xi_N}\right\}, \quad \gamma_{BF} \gg \max\left\{1, \frac{\rho_S\xi_S}{\rho_F\xi_F}\right\},$$

to neglect the suppression of superconductivity in S part of the proximity system. Here R_{B1}, R_{B2} and $\mathcal{A}_{B1}, \mathcal{A}_{B2}$ are the resistances and areas of the SN and SF interfaces; ξ_S, ξ_N, and ξ_F are the decay lengths of S, N, and F materials; while ρ_S, ρ_N, and ρ_F are their resistivities.

We assume that either temperature T is close to the critical temperature of superconducting electrodes T_c or parameters γ_{BN} and γ_{BF} are large enough to permit the use of the linearized Usadel equations in F and N films of the structure. Under the above conditions the problem of calculation of the critical current in the structure reduces to solution of the set of linearized Usadel equations,[21,61,62]

$$\xi_N^2\left\{\frac{\partial^2}{\partial x^2} + \frac{\partial^2}{\partial y^2}\right\}\Phi_N - \frac{|\omega|}{\pi T_c}\Phi_N = 0, \tag{1}$$

$$\xi_F^2\left\{\frac{\partial^2}{\partial x^2} + \frac{\partial^2}{\partial y^2}\right\}\Phi_F - \frac{\tilde{\omega}}{\pi T_c}\Phi_F = 0, \tag{2}$$

where $\xi_{N,F}^2 = (D_{N,F}/2\pi T_c)$, $D_{N,F}$ are the diffusion coefficients, $\omega = \pi T(2n+1)$ are the Matsubara frequencies, $\tilde{\omega} = |\omega| + iH \operatorname{sgn}\omega$, and H is the exchange integral of ferromagnetic material. The boundary conditions at SN and SF interfaces[63] are

$$\gamma_{BN}\xi_N\frac{\partial}{\partial y}\Phi_N = \pm G_0\Delta \exp\left\{\pm i\frac{\varphi}{2}\right\}, \quad y = L, 0, \tag{3}$$

$$\gamma_{BF}\xi_F\frac{\partial}{\partial y}\Phi_F = \pm \frac{\tilde{\omega}}{|\omega|}G_0\Delta \exp\left\{\pm i\frac{\varphi}{2}\right\}, \quad y = L, 0, \tag{4}$$

where L is the distance between superconducting electrodes, $G_0 = \omega/\sqrt{\omega^2+\Delta^2}$, and Δ is the modulus of the order parameter of superconducting electrodes.

At the FN interface ($x=0$) we also have[63]

$$\frac{\xi_N}{|\omega|}\frac{\partial}{\partial x}\Phi_N = \gamma\frac{\xi_F}{\tilde{\omega}}\frac{\partial}{\partial x}\Phi_F, \tag{5}$$

$$\gamma_B\xi_F\frac{\partial}{\partial x}\Phi_F + \Phi_F = \frac{\tilde{\omega}}{|\omega|}\Phi_N, \tag{6}$$

where $\gamma_B = R_{B3}\mathcal{A}_{B3}/\rho_F\xi_F$, $\gamma = \rho_N\xi_N/\rho_F\xi_F$, and R_{B3} and $\mathcal{A}_{B3}$ are the resistance and area of the NF interface. The boundary conditions at free interfaces,

$$\frac{\partial}{\partial x}\Phi_N = 0, \quad x = d_N, \tag{7}$$

$$\frac{\partial}{\partial x}\Phi_F = 0, \quad x = -d_F. \tag{8}$$

come from the demand of an absence of a current across them.

It is convenient to write the general solution of the boundary value problem (1)–(8) in the form[51]

$$\Phi_N(x,y) = \Phi_N(y) + \sum_{n=-\infty}^{\infty} A_n(x)\cos\frac{\pi n(y-L)}{L}, \tag{9}$$

$$\Phi_F(x,y) = \Phi_F(y) + \sum_{n=-\infty}^{\infty} B_n(x)\cos\frac{\pi n(y-L)}{L}, \tag{10}$$

where $\Phi_N(y)$ and $\Phi_F(y)$ are asymptotic solutions of Eqs. (9) and (10) at the distance far from FN interface,

$$\Phi_N(y) = \frac{G_0\Delta}{\sqrt{\Omega}\gamma_{BN}}\left(\frac{\cos\frac{\varphi}{2}\cosh\frac{L-2y}{2\xi_{N\Omega}}}{\sinh\frac{L}{2\xi_{N\Omega}}} - \frac{i\sin\frac{\varphi}{2}\sinh\frac{L-2y}{2\xi_{N\Omega}}}{\cosh\frac{L}{2\xi_N\Omega}}\right),$$

$$\Phi_F(y) = \frac{\sqrt{\tilde{\Omega}}G_0\Delta}{\Omega\gamma_{BF}}\left(\frac{\cos\frac{\varphi}{2}\cosh\frac{L-2y}{2\xi_{F\Omega}}}{\sinh\frac{L}{2\xi_{F\Omega}}} - \frac{i\sin\frac{\varphi}{2}\sinh\frac{L-2y}{2\xi_{F\Omega}}}{\cosh\frac{L}{2\xi_{F\Omega}}}\right),$$

where $\xi_{N\Omega} = \xi_N/\sqrt{\Omega}$, $\xi_{F\Omega} = \xi_F/\sqrt{\tilde{\Omega}}$, while functions $A_n(x)$ and $B_n(x)$ are solutions of appropriate one-dimensional boundary problem. The details of $A_n(x)$ and $B_n(x)$ determination are given in Appendix A.

Substitution of expressions (9) and (10) into the formula for the supercurrent I_S after routine calculations and several simplifications presented in Appendix B, Secs. B 1 and B 2, the most interesting from the practical point of view situation is when

$$H \gg \pi T_C, \quad \xi_F \ll \xi_N \tag{11}$$

results in $I_S = I_C \sin\varphi$, where

$$I_C = \frac{2\pi T}{e}\frac{d_N}{\xi_N}\frac{W}{\gamma_{BN}^2\rho_N}\operatorname{Re}\sum_{\omega>0}^{\infty}\frac{G_0^2\Delta^2}{\omega^2 q\xi_N\sinh(qL)}, \tag{12}$$

and the wave vector is given by

$$q = \frac{1}{\xi_N}\sqrt{\frac{\xi_N}{d_N}\frac{\gamma\sqrt{\tilde{\Omega}}}{\gamma_B\sqrt{\tilde{\Omega}} + \coth\left\{\frac{d_F}{\xi_F}\sqrt{\tilde{\Omega}}\right\}} + \Omega}. \tag{13}$$

It is necessary to note that in general the expression for the critical current except summation over ω contains also summation over infinite number of wave vectors which are the eigenvalues of boundary problem (1)–(8). As it is followed from estimations given in Appendix B, Sec. B 2 under the restrictions on the distance L between superconductors,

$$L \gg \mathrm{Re}\left(\frac{1}{q}\mathrm{arctanh}\frac{1}{\gamma_{BN} q \xi_N}\right) \tag{14}$$

and on thickness of the N layer,

$$\frac{\xi_F^2}{\eta h \xi_N^2} \ll \frac{d_N}{\xi_N} \ll \eta, \tag{15}$$

where

$$\eta = \begin{cases} \dfrac{1}{\gamma}\sqrt{\gamma_B^2 + \gamma_B\sqrt{2h^{-1}} + h^{-1}}, & \dfrac{d_F}{\xi_F} \gg 1/\sqrt{h} \\ \dfrac{1}{\gamma}\sqrt{\gamma_B^2 + 2\gamma_B \dfrac{\xi_F}{d_F}\dfrac{\Omega}{h^2} + \dfrac{\xi_F^2}{d_F^2 h^2}}, & \dfrac{d_F}{\xi_F} \ll 1/\sqrt{h}, \end{cases} \tag{16}$$

and $h = H/\pi T_C$ the main contribution to I_C comes from the item corresponding to the first eigenvalue q, which is given by expression (13) and for I_C one can get formula (12).

From Eq. (11) it follows that q weakly depends on temperature. As a result a change in temperature should weakly influence on decay length and period of I_C oscillations and mainly controls only the absolute value of the critical current (12). Neglecting in the first approximation the dependence of q on Matsubara frequency one can easily get $I_C(T) \propto f(T) = \Delta \tanh(\Delta/T)$. It is necessary to point out that the experimentally studied parameters such as decay length of I_C as a function of L and period of I_C oscillations should be mainly controlled by the real and the imaginary parts of wave vector q calculated at $\omega = \pi T$.

Below we will start with detailed examination of behavior of wave vector q as a function of geometrical and transport parameters of weak link. The calculated dependencies do not only provide the knowledge, which is necessary to take into account for the design of S/FNF/S structures with input properties, but also will be useful for understanding the features of $I_C(L, d_F)$ dependencies examined in the last paragraph of this paper.

III. PROPERTIES OF WAVE VECTOR q

In the limit of thin F film $d_F/\xi_F \ll 1/\sqrt{h}$ expression (13) for q transforms into the result obtained in Ref. 52 in the limit $\zeta_N \gg \zeta_F$,

$$q^2 = \frac{\Omega}{\xi_N^2} + \frac{(h^2 + \Omega^2)\zeta_F^2 + \Omega\xi_F^2 + ih\xi_F^2}{\zeta_N^2 \zeta_F^2 [h^2 + (\xi_F^2 \zeta_F^{-2} + \Omega)^2]}, \tag{17}$$

where $\zeta_F^2 = \gamma_B d_F/\xi_F$, $\zeta_N^2 = \gamma_B d_N/(\xi_N \gamma)$.

In the opposite case $d_F/\xi_F \gg 1/\sqrt{h}$ from Eq. (13) we get

$$q = \frac{1}{\xi_N}\sqrt{\Omega + \frac{\xi_N}{d_N}\gamma\sqrt{\frac{h}{2}}\frac{i + 1 + \sqrt{2}\gamma_B\sqrt{h}}{\sqrt{h}\gamma_B(\sqrt{2} + \gamma_B\sqrt{h}) + 1}}. \tag{18}$$

Below we will perform our analysis for $T = 0.5T_C$. At this temperature the main contribution into the critical current is provided by the term corresponding to the first Matsubara frequency ($n = 0$). For this reason in this paragraph we will study the properties of wave vector q for $\Omega = 0.5$ that is the value of Ω for ($n = 0$) and $T/T_C = 0.5$.

In Figs. 2 and 3 solid curves show the real and the imaginary parts of wave vector q as a function of d_F/ξ_F calculated from Eq. (13) for two ratios of normal film thickness $d_N/\xi_N = 0.01$ and $d_N/\xi_N = 0.1$. The dotted lines in these figures are the same dependencies, which are followed from asymptotic formula (17). All calculations were done for a set of parameters $\xi_N/\xi_F = 10$, $\gamma = 0.03$, $\gamma_B = 0.2$, and $h = 30$ which in accordance with analysis done in Ref. 52 provide the maximum value for imaginary part of q at $d_F/\xi_F = 0.1$, $d_N/\xi_N = 0.01$, and $d_N/\xi_N = 0.1$.

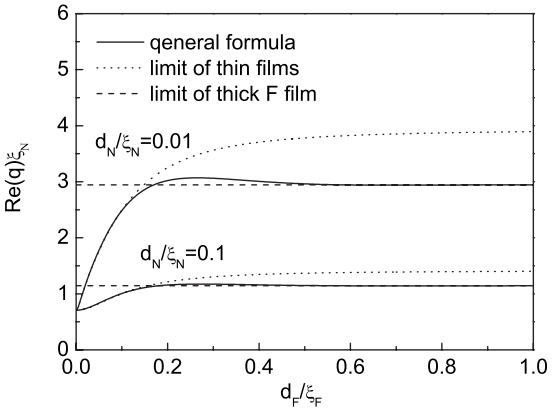

FIG. 2. Real part of q versus the thickness of F film d_F/ξ_F for two values of $d_N/\xi_N = 0.1, 0.01$ [solid lines for q calculated from Eq. (13), dotted lines for q calculated from formula for thin films (Ref. 52), and dashed lines correspond to the limit of thick F film (18)] at $\xi_N/\xi_F = 10$, $\Omega = 0.5$, $h = 30$, $\gamma_B = 0.2$, and $\gamma = 0.03$.

It is clearly seen that the solid and the dotted curves are in close agreement for $d_F/\xi_F \lesssim 0.1$. At $d_F/\xi_F \gtrsim 0.4$ the wave vector starts to be practically independent of d_F reaching the value determined by Eq. (18). This fact is very important from practical point of view. It says that the parameters of S/FN/S junctions do not deteriorate with increase in d_F, as it follows from the previously obtained[52] result (17) (see the dashed lines in Figs. 2 and 3). Moreover imaginary parts of q become very robust against the fluctuation of ferromagnetic film thickness in the practically important interval $d_F/\xi_F \gtrsim 0.4$. From Figs. 2 and 3 one can also see that taking into account finite value of thicknesses of films leads to some increase in decay length.

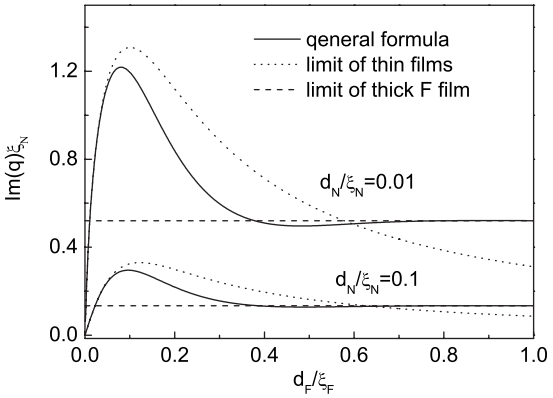

FIG. 3. Imaginary part of q versus the thickness of F film d_F/ξ_F for two values of $d_N/\xi_N = 0.1, 0.01$ [solid lines for q calculated from Eq. (13), dotted lines for q calculated from formula for thin films (Ref. 52), and dashed lines correspond to the limit of thick F film (18)] at $\xi_N/\xi_F = 10$, $\Omega = 0.5$, $h = 30$, $\gamma_B = 0.2$, and $\gamma = 0.03$.

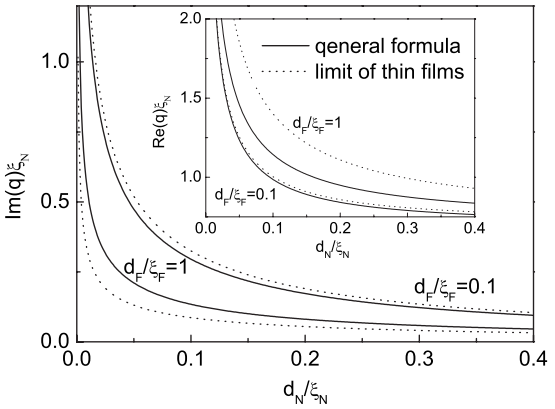

FIG. 4. Imaginary part of q versus the thickness of N film d_N/ξ_N for two values of $d_F/\xi_F=0.1,1$ [solid lines for q calculated from Eq. (13) and dotted lines for q calculated from formula for thin films (Ref. 52)] at $\xi_N/\xi_F=10$, $\Omega=0.5$, $h=30$, $\gamma_B=0.2$, and $\gamma=0.03$. Inset shows real part of q versus the thickness of N film d_N/ξ_N at the same parameters.

In Fig. 4 solid and dotted lines show the real and the imaginary parts of wave vector q as a function of d_N/ξ_N calculated from Eqs. (13) and (17), respectively, for two ratios of ferromagnetic film thickness $d_F/\xi_F=0.1$ and $d_F/\xi_F=1$ and at the same set of other parameters ($\xi_N/\xi_F=10$, $\gamma=0.03$, $\gamma_B=0.2$, $\Omega=0.5$, $h=30$).

From the data it follows that an increase in thickness of normal film leads to an increase in period of oscillations, which tends to infinity at large d_N. The decay length also increases with d_N and for $d_F/\xi_F=0.1$ it practically approaches the value $\xi_N/\sqrt{\Omega}$ that is the decay length of the single normal film.

Figures 5 and 6 show the real and the imaginary parts of wave vector q as a function of γ and γ_B calculated at $d_N/\xi_N=0.05$ for $\xi_N/\xi_F=10$, $\Omega=0.5$, and $h=30$. In Fig. 5, $\gamma_B=0.1$ and the inset shows the same dependencies calculated for $\gamma_B=0.01$. In Fig. 6, $\gamma=0.1,0.03$.

There is a significant discrepancy between the curves calculated from the general expression (13) for q and from

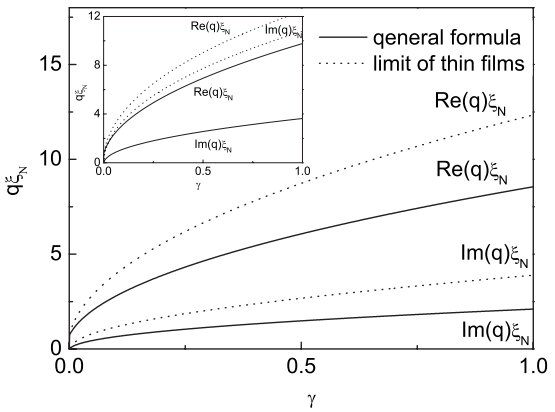

FIG. 5. Real and imaginary parts of q versus the parameter γ [solid lines for q calculated from Eq. (13) and dotted lines for q calculated from formula for thin films (Ref. 52)] at $\xi_N/\xi_F=10$, $\Omega=0.5$, $h=30$, $d_F/\xi_F=0.5$, $d_N/\xi_N=0.05$, and $\gamma_B=0.1$. Inset shows the same dependence at $\gamma_B=0.01$ and the same other parameters.

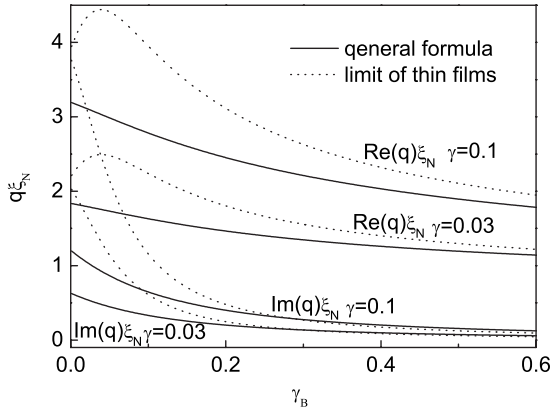

FIG. 6. Real and imaginary parts of q versus the parameter γ_B [solid lines for q calculated from Eq. (13) and dotted lines for q calculated from formula for thin films (Ref. 52)] at $\xi_N/\xi_F=10$, $\Omega=0.5$, $h=30$, $d_F/\xi_F=0.5$, $d_N/\xi_N=0.05$, and two values of $\gamma=0.1,0.03$.

asymptotic dependence (17) for q previously obtained in Ref. 52. This discrepancy is larger, the smaller is the suppression parameter γ_B. This result is obvious since expression (17) is not valid at small γ_B. From direct comparison of the curves we can conclude that in practically important range of $\gamma \gtrsim 0.1$ within the accuracy of 20% we may use the results of Refs. 52–54 for $\gamma_B \gtrsim 0.2$.

Figure 7 shows the dependencies of real and imaginary parts of q upon thickness of F film calculated for $\xi_N/\xi_F=10$, $\Omega=0.5$, $h=30$, $\gamma=0.03$, and $d_N/\xi_N=0.05$ and the set of parameters $\gamma_B=0.2,0.1,0.01$ (solid, dashed, and dotted lines, respectively). Inset in this figure shows the same dependencies obtained for smaller value of exchange energy $h=5$. It is clearly seen that $\mathrm{Im}(q)$ has a maximum as a function of d_F/ξ_F. The position of the maximum shifts to larger F layer thickness with γ_B decrease. At $\gamma_B=0.2$ the maximum of imaginary part has the value $\max[\mathrm{Im}(q)]\approx 0.5\xi_N$, which is achieved at $d_F/\xi_F\approx 0.1$. For smaller suppression parameters $\gamma_B=0.1$ ($\gamma_B=0.01$) the maximum of imaginary part equals to $\mathrm{Im}(q)\approx 2/3\xi_F$ ($\max[\mathrm{Im}(q)]\approx\xi_F$) and is achieved at $d_F/\xi_F\approx 0.13$ and $d_F/\xi_F\approx 0.2$, respectively. Inset in Fig. 7 also

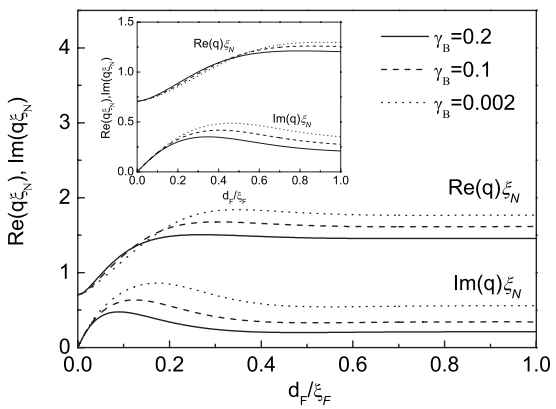

FIG. 7. Imaginary and real parts of q versus the thickness of F film d_F/ξ_F for $\gamma_B=0.2,0.1,0.01$ (solid, dashed, and dotted lines) at $\xi_N/\xi_F=10$, $\Omega=0.5$, $h=30$, $\gamma=0.03$, and $d_N/\xi_N=0.05$. Inset shows the same dependence for $h=5$.

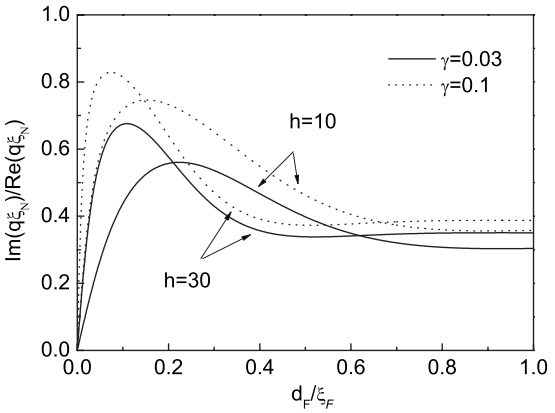

FIG. 8. Ratio of imaginary part of q to its real part versus the thickness of F film d_F/ξ_F for two values of $\gamma=0.03, 0.1$ (solid and dotted lines) at $\xi_N/\xi_F=10$, $\gamma_B=0.01$, $d_N/\xi_N=0.05$, $\Omega=0.5$, and $h=30, 10$.

demonstrates that both position of the maximum of $\mathrm{Im}(q)$ and its absolute value depend on exchange energy h. Decrease in h shifts $\max[\mathrm{Im}(q)]$ to larger ratio d_F/ξ_F and simultaneously suppresses the value of this maximum. From the structure of expression (13) for q it follows that its imaginary part $\mathrm{Im}(q)$ has a maximum as a function of exchange energy h. Indeed, at $h\to 0$ the period of $I_C(L)$ oscillation tends to infinity, which is equivalent to $\mathrm{Im}(q)\to 0$ At large h the imaginary part $\mathrm{Im}(q)\propto h^{-1/2}$ that is also goes to zero with h increase. At $d_F/\xi_F \gtrsim 0.4$ both $\mathrm{Im}(q)$ and $\mathrm{Re}(q)$ saturate and practically become independent on F layer thickness.

Figure 8 shows the dependence of $\mathrm{Im}(q)/\mathrm{Re}(q)$ as a function of d_F/ξ_F. The calculations have been done for $\gamma_B=0.01$, $\xi_N/\xi_F=10$, $\Omega=0.5$, and for two values of suppression parameter $\gamma=0.03$ (solid line) and $\gamma=0.01$ (dotted line). The values of exchange energy h have been equal to 10 and 30, as it is marked in Fig. 8 by arrows. The curves presented in Fig. 8 can be also used for minimization of period of I_C oscillations. Actually, the maximum of the ratio $\mathrm{Im}(q)/\mathrm{Re}(q)$ corresponds to the minimum decay per one period. It is obvious that this maximum is located near maximum of $\mathrm{Im}(q)$. Therefore the position of this maximum shifts to smaller d_F with increase in exchange energy or suppression parameter γ.

If we want to fix the value of $\max[\mathrm{Im}(q)]$ in the vicinity of ξ_N and to shift this maximum to the largest d_F, we should choose suppression parameter γ_B in the range of 0.01 (for large d_F) and perform the fitting procedure in order to estimate suppression parameter γ and exchange energy h. For instance, we may find that for $h=30$ maximum of $\mathrm{Im}(q)$ is on the order of ξ_N and it is achieved for $\gamma=0.03$ at $d_F/\xi_F \approx 0.18$, while for $h=10, \gamma=0.03$ the maximum is shifted to $d_F/\xi_F \approx 0.3$. The smaller the exchange energy, the thicker should be the thickness of F film to get $\mathrm{Im}(q)$ in the range of ξ_N. Thus for $h=5, \gamma=0.09$ the maximum is achieved at $d_F/\xi_F=0.45$. From the data presented in Figs. 7 and 8 it follows that for all mentioned above sets of parameters the ratio $\mathrm{Im}(q)/\mathrm{Re}(q)\approx 0.6$ and does not exceed this value. For thick F film $d_F/\xi_F \gg 1/\sqrt{h}$ the maximum of $\mathrm{Im}(q)/\mathrm{Re}(q)$ is achieved at small $\gamma_B\to 0$, $h\gg\Omega$, and $\gamma\xi_N/d_N\sqrt{h/2}\gg\Omega$ and this maximum relation is $\mathrm{Im}(q)/\mathrm{Re}(q)\sim 0.4$.

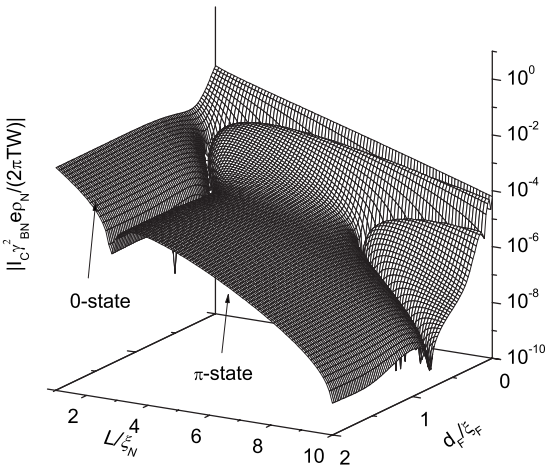

FIG. 9. Normalized absolute value of critical current versus the thickness of F film d_F/ξ_F and distance between the superconducting electrodes L/ξ_N for $\gamma=0.03$, $\gamma_B=0.01$, $\xi_N/\xi_F=10$, $d_N/\xi_N=0.05$, $h=10$, $\gamma_{BN}/\gamma_{BF}=1$, and $T=0.5T_C$.

IV. THICKNESS DEPENDENCE OF THE CRITICAL CURRENT

We consider that the critical current 12 of the studied S/FN/S Josephson junction (see Fig. 9) is a function of two arguments. They are the distance between superconducting electrodes L/ξ_N and the thickness of ferromagnetic film d_F/ξ_F. The dependence of $I_C(L/\xi_N, d_F/\xi_F)$ has shown in Fig. 9. It has been calculated from Eqs. (12) and (13) for $h=10$, $d_N/\xi_N=0.05$, $\gamma_B=0.01$, $\gamma=0.03$, $\gamma_{BF}/\gamma_{BN}=1$, and $T=0.5T_C$.

In the limit $d_F\to 0$ the period of critical current oscillations tends to infinity (see Fig. 9) and I_C decays monotonically with L, as it must be for S/N/S Josephson junctions. With d_F increasing (see Fig. 10) the dependence of critical current as a function of L/ξ_N has the form of damped oscillations. The decay length of these oscillations is different for different thicknesses of F film. The most intensive suppression is localized in the vicinity of $d_F/\xi_F\approx 0.6$ since $\mathrm{Re}(q)$ has maximum at this thickness of F layer. It is seen that the

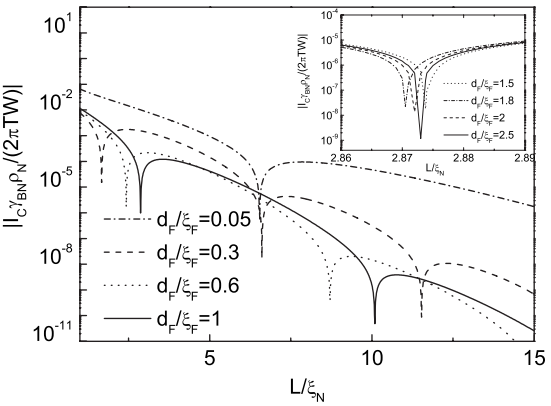

FIG. 10. Normalized absolute value of critical current versus the distance between electrodes L/ξ_N for $\gamma=0.03$, $\gamma_B=0.01$, $\xi_N/\xi_F=10$, $d_N/\xi_N=0.05$, $h=10$, $\gamma_{BN}/\gamma_{BF}=1$, and $T=0.5T_C$ for several thicknesses of F film $d_F/\xi_F=0.05, 0.3, 0.6, 1$. Insert shows the same dependence for $d_F/\xi_F=1.5, 1.8, 2, 2.2$.

suppression of I_C is smaller for thicker ($d_F > 0.6\xi_F$) and thinner ($d_F < 0.6\xi_F$) F films. The period of I_C oscillations decreases with d_F achieving the smallest value at $d_F/\xi_F \approx 0.3$. Further increase in d_F results in increase in this period. Finally in the range of thickness $d_F/\xi_F > 0.5$ both period of I_C oscillations and decay length are nearly constant. In the interval of F layer thickness $d_F/\xi_F \gtrsim 1$ the position of zeros of $I_C(L,d_F)$ undergoes oscillations as a function of d_F (see inset in Fig. 10). They take place around values $L=L_n$, under which $I_C(L_n,d_F)=0$ at $d_F \gg \xi_F$. The amplitude of these oscillations decays with increase in d_F. It is interesting to mention that the larger is the L_n, the more intensive are the amplitudes of the oscillations. This behavior can be easily understood from the form of $q(d_F)$ dependence (13). In the vicinity of $L=L_n$ the critical current is small due to the 0-π transition of I_C as a function of L. Under this condition any small variations in q, which occur due to factor $\coth(d_F\sqrt{\tilde{\Omega}}/\xi_F)$ in Eq. (13), start to become important giving rise to the discussed $I_C(L,d_F)$ behavior.

Figure 11 shows the $I_C(L,d_F)$ dependencies calculated at fixed values of L under $h=10$, $d_N/\xi_N=0.05$, $\gamma_B=0.01$, $\gamma=0.03$, $\gamma_{BF}/\gamma_{BN}=1$, and $T=0.5T_C$.

In the small L domain the properties of the S/FN/S junction do not depend on the structure of weak link region. The critical current I_C is practically independent on d_F, so that there is no transition from zero to π state on $I_C(d_F)$. With the increase in L the $I_C(d_F)$ dependence becomes apparent (see Fig. 9) resulting in suppression of I_C. This suppression is different for different thicknesses of F film. The strongest suppression is realized in the vicinity of $d_F/\xi_F \approx 0.3$. This fact is illustrated in Fig. 11(a) by the line corresponding to the ratio $L/\xi_N=1.3$. It is seen that at this value of L/ξ_N the suppression of I_C is smaller for thicker ($d_F > 0.3\xi_F$) and thinner ($d_F < 0.3\xi_F$) F films. At $L/\xi_N \approx 1.67$ and $d_F \approx 0.3\xi_F$ the magnitude of critical current for the first time reaches zero, while the sign of I_C does not change.

With further increase in L the $L/\xi_N, d_F/\xi_F$ plane starts to be subdivided into two regions separated by the line along which the junction critical current is equal to zero. The boundary between the regions has two branches (see Fig. 12). The first one is located at $d_F < 0.3\xi_F$. It starts from the first critical point $(L_{c1}/\xi_N, d_{F,c1}/\xi_F) \approx (1.67, 0.3)$ and $d_{F,c1}$ is smaller the larger the L is. The second branch is located at $d_F > 0.3\xi_F$. It starts from the same critical point and for large d_F asymptotically verges toward the line $L=L_1$ exhibiting damped oscillation around it. As a result, any cross section presented in Fig. 9 dependence of $I_C(L/\xi_N, d_F/\xi_F)$ by a perpendicular to L axis plane in the region $1.67 < L/\xi_N < 2.87$ should give a dependence of $I_C(d_F)$ having the typical shape shown by solid line ($L/\xi_N=1.8$) in Fig. 11(a). It demonstrates that in this range of distances between S electrodes ($1.67 < L/\xi_N < 2.87$) for any given L there is a nucleation of only one π state in between of two zero states in $I_C(d_F)$ dependence. The interval of d_F, in which the π state exists, becomes wider the larger the L. Note also that for $1.67 < L/\xi_N < 2.87$ only the zero state can be realized for large $d_F/\xi_F \gtrsim 0.8$.

The number of transitions between zero and π states in $I_C(d_F)$ increases by asymptotically approaching the line $L = L_1$. This is illustrated in Fig. 11(b). At $L/\xi_N=2.6$ there are still only two transitions, namely, from zero to π state and from π to zero state. At $L/\xi_N \approx 2.8702$ in the zero state domain there is nucleation of the next critical point at $d_F/\xi_F \approx 1.7$. In it $I_C=0$, while the sign of I_C is kept positive for all $d_F/\xi_F \gtrsim 0.8$. Further increase in L leads to generation of additional π state in the vicinity of $d_F/\xi_F \approx 1.7$ as it is shown in Fig. 11(b) by solid line. The closer L to L_1 the larger is the amount of zero to π transitions. As it was already pointed above, this behavior of critical current at $L/\xi_N \approx L_1$ is a result of small oscillations of $\mathrm{Im}(q)$ which occur at large d_F. Note that in the region $L=L_1-0$ S/FN/S junction always is in the zero state at $d_F \to \infty$.

Contrary to that, for $L=L_1+0$ it is π state that is finally established in the limit of large d_F [see the dotted line for $L/\xi_N=2.8729$ in Fig. 11(c)]. Further increase in L leads to the reduction in thickness intervals in which the zero states exists. They collapse one by one with L. The last stage of this process is shown in Fig. 11(c). It is seen that transition from

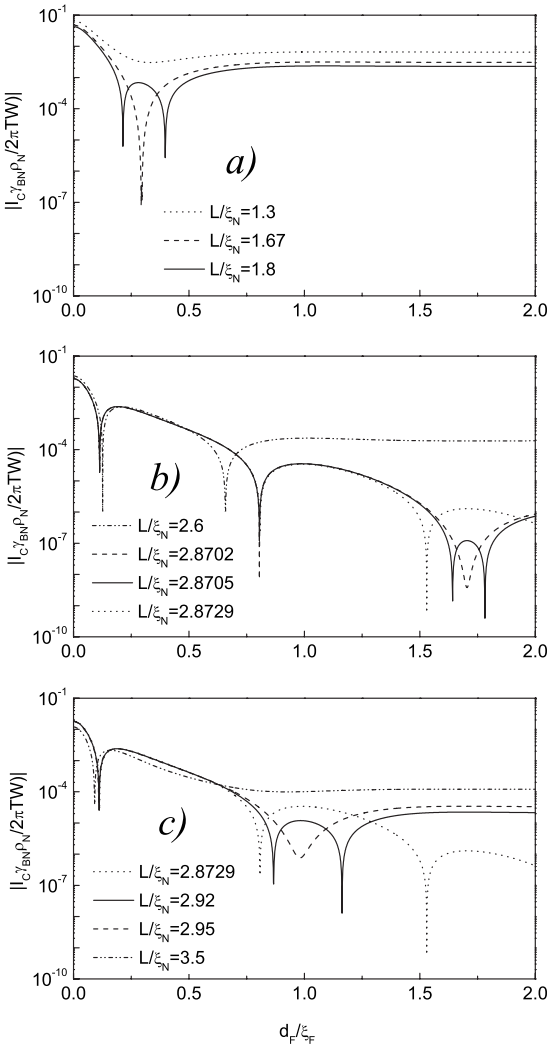

FIG. 11. Normalized absolute value of critical current versus the thickness of F film d_F/ξ_F for $\gamma=0.03$, $\gamma_B=0.01$, $\xi_N/\xi_F=10$, $d_N/\xi_N=0.05$, $h=10$, $\gamma_{BN}/\gamma_{BF}=1$, and $T=0.5T_C$ for several distances between the superconducting electrodes $L/\xi_N=1.3, 1.67, 1.8, 2.6, 2.8702, 2.8705, 2.8729, 2.95, 2.95, 3.5$.

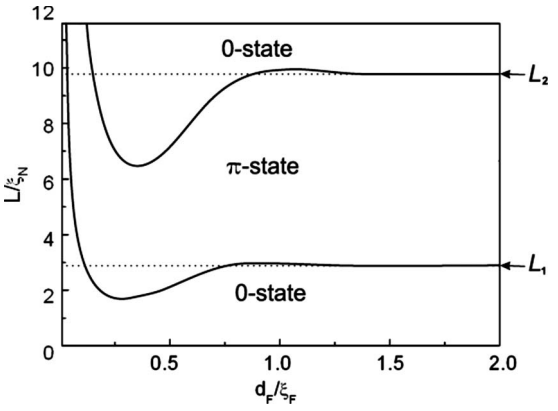

FIG. 12. The (L,d_F) phase diagram for S/FN/S junction at $\gamma=0.03$, $\gamma_B=0.01$, $\xi_N/\xi_F=10$, $d_N/\xi_N=0.05$, $h=10$, $\gamma_{BN}/\gamma_{BF}=1$, and $T=0.5T_C$.

$L/\xi_N=2.8729$ to $L/\xi_N=2.92$ leads to reduction in the zero state located in the vicinity of $d_F/\xi_F=1$. At $L/\xi_N\approx 2.95$ it completely shrinks, so that I_C becomes always negative at $d_F/\xi_F\gtrsim 0.2$. As a result in the distance interval $3.5\lesssim L/\xi_N\lesssim 6.5$ the typical shape of $I_C(d_F)$ dependence for a fixed L has the form of the curve presented in Fig. 11(c) by the line calculated for $L/\xi_N\approx 3.5$. There is only one 0-π transition, which occurs at $d_F/\xi_F\approx 0.2$. It is the first branch of the locus of point at which $I_C=0$ on $L/\xi_N, d_F/\xi_F$ plane.

It is seen from Figs. 9 and 12 that at $L/\xi_N\approx 6.5$ and $d_F/\xi_F\approx 0.32$ there is a nucleation of the next critical point. Again the two branches start to propagate from it. They produce the next boundary on $L/\xi_N, d_F/\xi_F$ plane, thus subdividing this plane into three regions.

The first branch is located at $d_F/\xi_F\lesssim 0.32$. It propagates along L nearly parallel to the already existing in this domain branch generated at critical point $(L_{c1}/\xi_N, d_{F,c1}/\xi_F)\approx(1.67, 0.3)$. In the narrow zone between these branches the junction is in the π state. The second branch is located at $d_F>0.32\xi_F$. Starting from the second critical point for large d_F it asymptotically verges toward the line $L=L_2=10.089$ exhibiting damped oscillations around it. Quantitatively the behavior of $I_C(L,d_F)$ in the vicinity of $L=L_2$ and at slightly larger L is the same as we discuss above. There is increasing number of zero to π transitions as soon as $L\to L_2-0$ and the collapses of π states in the $L=L_2+0$ region with L increase. Finally in the interval $10.32\lesssim L/\xi_N\lesssim 11.5$ there are only two transitions of $I_C(d_F)$ and at $d_F/\xi_F\gtrsim 0.012$ there is only zero state of the critical current.

V. CONCLUSION

We have studied the Josephson effect in S/FN/S structures under condition of relatively large suppression parameters γ_{BN} and γ_{BF} at SN and SF interfaces. We have derived the general expression for the critical current of these structures, applicable for arbitrary values of suppression parameters at FN interface and in the practically important case of relatively thin normal film (B16), (B20), and arbitrary thickness of a ferromagnetic layer. It is shown that the critical current of the junction, I_C, exhibits damped oscillations as a function of a distance L between S electrodes. We have discussed the dependencies of the oscillation period and the decay length of $I_C(L)$ on the NF interface parameters and on F and N layers thicknesses. We have demonstrated that for typical values of exchange energy $h\approx 30$ and in the limit of thin F and N layers ($d_F\lesssim 0.1\xi_F$ and $d_N\lesssim\xi_N$) the results obtained for the critical current cross over to that previously derived in Ref. 52. It is qualitatively clear that the considerations performed in Refs. 53 and 54 for more sophisticated S/FNF/S Josephson junctions are also valid in this parameter range.

Further increase in d_N results in increase in both period of $I_C(L)$ oscillations and its decay length. The 0-π transition point shifts to larger L, so that the properties of the structure continuously transform into those of SNS devices.

Increase in d_F is accompanied by more complicated processes. The period of I_C oscillations and the decay length have minima as a function of d_F. The maximum value of d_F at which these minima can be achieved for typical values of h is $d_F/\xi_F\lesssim 0.6$.

In the practically interesting range of F layer thickness $d_F\gtrsim\xi_F$ the dependence of $I_C(L)$ is qualitatively the same as previously found in Ref. 52. There is a continuous transition from zero to π state with increase in L. Noticeable exceptions are narrow intervals of L located in the vicinity of $L=L_n$, where L_n is the distance at which $I_C(L_n,d_F)=0$ for $d_F\gg\xi_F$ (see inset in Figs. 10 and 11). In these intervals the position of the point at which $I_C=0$ exhibits damping oscillations as a function of d_F and the number of transitions from 0 to π state in $I_C(L,d_F)$ increases under $L\to L_n$. Outside these intervals sign and value of I_C are independent on d_F for $d_F\gtrsim\xi_F$. This fact is very important for possible applications of S/FN/S Josephson junctions and S/FNF/S spin valve Josephson devices.

Our calculations have shown that to fabricate the proposed S/FNF/S structures it is favorable to have the thickness of the N film in the range $d_N\approx 0.1\xi_N-0.2\xi_N$. For typical decay length of high-conductivity metals, ξ_N, on the order of 100 nm, this restriction results in $d_N\approx 10-20$ nm. This range of d_N thicknesses is ordinarily used in fabricating SNS Josephson devices. In our particular case this interval of thicknesses provides the required coupling strength between the polarized electron subsystems in the two F films, and simultaneously such d_N range is sufficient to support superconducting correlations induced into from the S electrodes.

From the data presented in Fig. 6 it also follows that the smaller is the suppression parameter γ_B at the FN interface, the smaller is the decay length of I_C and the period of its oscillations. Typical values of specific boundary resistance at a sharp metal interface,[64] $R_B\mathcal{A}\approx 10^{-11}$ Ω cm^2, and typical values of $\rho_F\xi_F$ product are close to each other resulting in $\gamma_B\lesssim 1$. Increase in γ_B does not strongly influence the decay length, which tends to ξ_N when γ_B goes to infinity. Contrary to that, the period of I_C oscillations depends stronger on γ_B. It goes to infinity in the limit of large γ_B, thus preventing the experimental observation of zero to π transition. Therefore we may conclude that the smaller is the suppression parameter γ_B, the stronger is the interaction of polarized electrons in the N film of S/FNF/S junctions and the better are the conditions for realization of effects predicted in Refs. 52–54.

It is also necessary to note that in our calculations we have chosen the suppression parameter γ equal to 0.03 or

0.1. For small γ_B, this suppression parameter has to be small in order to prevent strong suppression of superconductivity induced into N film due to the proximity with the F films. For $\gamma \lesssim 0.1$ the superconducting correlations in the F films are supported due to the proximity effect, and the back influence of F films on superconductivity in the N part of FNF trilayer is small. The conclusion about smallness of γ comes also from inequality (15). For $d_N/\xi_N \approx 0.1$, $d_F/\xi_F \approx 1$, $h \approx 30$, and $\gamma_B \to 0$ the rough estimate from inequality (15) gives $\gamma \ll 1$. The restriction $\gamma \lesssim 0.1$ is not too strong since for typical values of $\rho_N \xi_N$ and $\rho_F \xi_F$ products their ratio just provides the necessary small values for the γ parameter.

Finally, our analysis shows that for practically interesting interval of F layer thickness $d_F \gtrsim \xi_F$ the parameters of S/FNF/S spin valve devices are very robust to variations in d_F if the distance between superconductors is not very close to the critical points L_n, at which the $I_C=0$. In the last few years, noticeable progress was achieved in the development of special techniques for fabricating superconducting spintronic devices based on SF structures. Among them are arrays of Nb/CuNi π junctions,[65] S/F1/N/F2 spin valves consisting on V/Fe superlattices,[60] Nb/CuNi nanostructures with a high-quality SF interface, exhibiting re-entrant and double re-entrant $T_C(d_F)$ behaviors.[66,67] We are convinced that these experimental developments together with theoretical considerations performed in this work and in Refs. 52–54 provide a good background for fabrication of new class of Josephson spintronic devices.

ACKNOWLEDGMENTS

This work was supported by NanoNed Program under Project No. TCS7029, RFBR Project No. 08-02-90012, and Russian State Contract No. -133.2008.2.

APPENDIX A

1. Solution of linearized Usadel equations

It is convenient to write the general solution of the boundary value problem (1)–(8) in the form

$$\Phi_N(x,y) = \Phi_N(y) + \sum_{n=-\infty}^{\infty} A_n(x)\cos\frac{\pi n(y-L)}{L}, \quad \text{(A1)}$$

$$\Phi_F(x,y) = \Phi_F(y) + \sum_{n=-\infty}^{\infty} B_n(x)\cos\frac{\pi n(y-L)}{L}, \quad \text{(A2)}$$

where $\Phi_N(y)$ and $\Phi_F(y)$ are asymptotic solutions of Eqs. (1) and (2) at the distance far from FN interface,

$$\Phi_N(y) = \frac{G_0\Delta}{\sqrt{\Omega}\gamma_{BN}}\left(\frac{\cos\frac{\varphi}{2}\cosh\frac{L-2y}{2\xi_{N\Omega}}}{\sinh\frac{L}{2\xi_{N\Omega}}} - \frac{i\sin\frac{\varphi}{2}\sinh\frac{L-2y}{2\xi_{N\Omega}}}{\cosh\frac{L}{2\xi_N\Omega}}\right),$$

$$\Phi_F(y) = \frac{\sqrt{\tilde{\Omega}}G_0\Delta}{\Omega\gamma_{BF}}\left(\frac{\cos\frac{\varphi}{2}\cosh\frac{L-2y}{2\xi_{F\Omega}}}{\sinh\frac{L}{2\xi_{F\Omega}}} - \frac{i\sin\frac{\varphi}{2}\sinh\frac{L-2y}{2\xi_{F\Omega}}}{\cosh\frac{L}{2\xi_{F\Omega}}}\right),$$

where $\xi_{N\Omega}=\xi_N/\sqrt{\Omega}$, $\xi_{F\Omega}=\xi_F/\sqrt{\tilde{\Omega}}$, while functions $A_n(x)$ and $B_n(x)$ satisfy the following boundary problem:

$$\xi_N^2\frac{\partial^2}{\partial x^2}A_n(x) - u_n^2 A_n(x) = 0, \quad \text{(A3)}$$

$$\xi_F^2\frac{\partial^2}{\partial x^2}B_n(x) - v_n^2 B_n(x) = 0, \quad \text{(A4)}$$

$$\frac{\gamma_B}{\gamma}\xi_N\frac{\tilde{\Omega}}{\Omega}\frac{\partial}{\partial x}A_n(0) - \frac{\tilde{\Omega}}{\Omega}A_n(0) + B_n(0) = R_n, \quad \text{(A5)}$$

$$\gamma_B\xi_F\frac{\partial}{\partial x}B_n(0) + B_n(0) - \frac{\tilde{\Omega}}{\Omega}A_n(0) = R_n, \quad \text{(A6)}$$

$$R_n = \frac{\tilde{\Omega}}{\Omega}\frac{G_0\Delta}{L}\kappa_n[e^{i\varphi/2} + (-1)^n e^{-i\varphi/2}], \quad \text{(A7)}$$

$$\frac{\partial}{\partial x}A_n(d_N) = 0, \quad \frac{\partial}{\partial x}B_n(-d_F) = 0. \quad \text{(A8)}$$

Here $\Omega=|\omega|/\pi T_C$, $\tilde{\Omega}=\tilde{\omega}/\pi T_C$, and

$$\kappa_n = \frac{1}{\gamma_{BN}}\frac{\xi_N}{u_n^2} - \frac{1}{\gamma_{BF}}\frac{\xi_F}{v_n^2}, \quad \text{(A9)}$$

$$u_n = \sqrt{\left(\frac{\pi n\xi_N}{L}\right)^2 + \Omega}, \quad v_n = \sqrt{\left(\frac{\pi n\xi_F}{L}\right)^2 + \tilde{\Omega}}. \quad \text{(A10)}$$

Solution of Eqs. (A3)–(A8) has the form

$$A_n(x) = -\frac{R_n\gamma v_n\Omega\cosh\left\{\frac{x-d_N}{\xi_N}u_n\right\}}{\tilde{\Omega}\delta_n\sinh\frac{u_n d_N}{\xi_N}}, \quad \text{(A11)}$$

$$B_n(x) = \frac{R_n u_n\cosh\left\{\frac{x+d_F}{\xi_F}v_n\right\}}{\delta_n\sinh\frac{v_n d_F}{\xi_F}}, \quad \text{(A12)}$$

where δ_n is defined as

$$\delta_n = \gamma_B v_n u_n + u_n\coth\frac{v_n d_F}{\xi_F} + \gamma v_n\coth\frac{u_n d_N}{\xi_N}. \quad \text{(A13)}$$

APPENDIX B

1. Calculation of supercurrent across S/FN/S junction

To calculate the supercurrent across the S/FN/S junction we substitute expressions (A1), (A2), and (A11)–(A13) into

formula for the general formula for supercurrent,

$$I_S(x,y) = \frac{-i\pi TW}{e\rho_F}\sum_{\omega=-\infty}^{\infty}\frac{1}{\tilde{\omega}^2}\int_{-d_f}^{0}\left[\Phi^*_{-\omega,F}\frac{\partial}{\partial y}\Phi_{\omega,F}\right] - \frac{i\pi TW}{e\rho_N}\sum_{\omega=-\infty}^{\infty}\frac{1}{\omega^2}\int_{0}^{d_n}\left[\Phi^*_{-\omega,N}\frac{\partial}{\partial y}\Phi_{\omega,N}\right].$$

The calculations gives $I_S = I_C \sin\varphi$, where

$$I_C = \frac{\Delta^2\pi TW\gamma}{e\rho_N}\sum_{\omega=-\infty}^{\infty}\frac{G_0^2}{\omega^2}\left[\sum_{j=1}^{6}k_jS_j + \frac{d_F}{\sqrt{\tilde{\Omega}}\xi_N\gamma_{BF}^2\sinh\frac{L}{\xi_{F\Omega}}} + \frac{d_N/\gamma}{\sqrt{\Omega}\xi_N\gamma_{BN}^2\sinh\frac{L}{\xi_{N\Omega}}}\right] \quad \text{(B1)}$$

and W is a width of junction in the direction perpendicular to axes $0y$ and $0x$. The last two items in Eq. (B1) determine the critical current of the structures with either ferromagnetic (SFS) or normal (SNS) interlayers.[21,62,68,69] By S_j we define the ordinary and the double sums as follows:

$$S_1 = \sum_{n=-\infty}^{\infty}\frac{n\kappa_n u_n \sin\frac{\pi n}{2}}{v_n\delta_n}, \quad S_2 = \sum_{n=-\infty}^{\infty}\frac{n\kappa_n v_n \sin\frac{\pi n}{2}}{u_n\delta_n},$$

$$S_3 = \sum_{n=-\infty}^{\infty}\frac{\kappa_n u_n \cos\frac{\pi n}{2}}{v_n\delta_n}, \quad S_4 = \sum_{n=-\infty}^{\infty}\frac{\kappa_n v_n \cos\frac{\pi n}{2}}{u_n\delta_n},$$

$$S_5 = \sum_{n,m=-\infty}^{\infty}\frac{C_{nm}u_nu_m}{\sinh\frac{v_nd_F}{\xi_F}\sinh\frac{v_md_F}{\xi_F}}I_v,$$

$$S_6 = \sum_{n,m=-\infty}^{\infty}\frac{C_{nm}v_nv_m}{\sinh\frac{u_md_N}{\xi_N}\sinh\frac{u_nd_N}{\xi_N}}I_u,$$

$$I_v = \frac{\sinh\frac{(v_n+v_m)d_F}{\xi_F}}{v_n+v_m} + \frac{\sinh\frac{(v_n-v_m)d_F}{\xi_F}}{v_n-v_m},$$

$$I_u = \frac{\sinh\frac{(u_n+u_m)d_N}{\xi_N}}{u_n+u_m} + \frac{\sinh\frac{(u_n-u_m)d_N}{\xi_N}}{u_n-u_m},$$

$$C_{nm} = \frac{n\sin\frac{\pi n}{2}\cos\frac{\pi m}{2}\kappa_m\kappa_n}{\delta_m\delta_n}, \quad \text{(B2)}$$

and coefficients k_j are

$$k_1 = \frac{\sqrt{\tilde{\Omega}}\xi_{F\Omega}^2\pi}{\gamma_{BF}L^2\sinh\frac{L}{2\xi_{F\Omega}}}, \quad k_2 = \frac{-\sqrt{\Omega}\xi_{N\Omega}^2\pi}{\gamma_{BN}L^2\sinh\frac{L}{2\xi_{N\Omega}}},$$

$$k_3 = \frac{\sqrt{\Omega}\xi_{N\Omega}^2\pi}{\gamma_{BN}L^2\sinh\frac{L}{2\xi_{N\Omega}}}, \quad k_4 = \frac{-\xi_N}{\gamma_{BN}L\cosh\frac{L}{2\xi_N\Omega}},$$

$$k_5 = \frac{\pi\xi_N\xi_F^2}{L^3}, \quad k_6 = \gamma\frac{\pi\xi_N^3}{L^3}. \quad \text{(B3)}$$

Expressions (B1)–(B3) are the main mathematical result of this work and are the subject of more detailed analysis given below. They give the general expression for the critical current of S-FN-S Josephson structure.

2. Critical current of S/FN/S junction

To calculate sums (B2) we may use the procedure known from the theory of functions of complex variables,

$$\sum_{n=-\infty}^{\infty}f(n)\sin(\pi n/2) = \frac{\pi}{2}\sum_k\frac{\mathrm{res}[f(z_k)]}{\cos(\pi/2z_k)}, \quad \text{(B4)}$$

$$\sum_{n=-\infty}^{\infty}f(n)\cos(\pi n/2) = -\frac{\pi}{2}\sum_k\frac{\mathrm{res}[f(z_k)]}{\sin(\pi/2z_k)}, \quad \text{(B5)}$$

where $\mathrm{res}[f(z_k)]$ is residue of function $f(z)$ at the critical point z_k. From Eq. (B2) it follows that there are critical points $z_u = \pm iL\sqrt{\Omega}/(\xi_N\pi)$ and $z_v = \pm iL\sqrt{\tilde{\Omega}}/(\xi_F\pi)$, which are the roots of equations $u(z)=0$ and $v(z)=0$, respectively. In addition there is also an infinite number of z_k, which are the roots of the equation

$$\delta(z) = 0. \quad \text{(B6)}$$

Applying procedures (B4) and (B5) to calculation of Eq. (B2) it is possible to show that the last two terms in expression for I_C (B1) are exactly compensated by the parts of these sums, which are calculated from the residue at critical points $z=z_u$ and $z=z_v$. Therefore critical current (B1) can be expressed as the sum of terms resulting from the application of rules (B4) and (B5) to Eq. (B2) at $z=z_k$.

Our analysis have shown that the value part of z_k consists of a root having the lowest real part, $z=z_{min}$, and the two systems of roots. In the first system, $z_{k,N}$, there is an item in the real part of $z_{k,N}$, which at large k increases with the number k of the root as $k\xi_N/d_N$; while in the second, $z_{k,F}$, this increase is proportional to $k\xi_F/d_F$. Below we will restrict ourselves to the consideration of the limit at which z_{min} makes the major contribution to the junction critical current, i.e., $|z_{min}| \ll |z_k|$. It can be shown that the lowest value among the roots of $z_{k,F}$ group is achieved at the limit of large d_F and is bounded by $\sqrt{\tilde{\Omega}}L/(\pi\xi_F)$. The lowest value of second group of the roots, $z_{k,N}$, is bounded by $\sqrt{\xi_N^2/d_N^2-\Omega}[L/(\pi\xi_N)]$, the value at which $z_{k,N}$ are approached in the limit of small γ. Thus under the condition

$$|z_{min}| \ll |\sqrt{\tilde{\Omega}}L/(\pi\xi_F)|, \quad \text{(B7)}$$

$$|z_{min}| \ll |\sqrt{\xi_N^2/d_N^2-\Omega}[L/(\pi\xi_N)]|, \quad \text{(B8)}$$

we can rewrite Eq. (B6) in the form

$$u^2 = -\frac{\xi_N}{d_N}\frac{\gamma\sqrt{\tilde{\Omega}}}{\gamma_B\sqrt{\tilde{\Omega}}+\coth\left\{\frac{d_F}{\xi_F}\sqrt{\tilde{\Omega}}\right\}}, \quad \text{(B9)}$$

and for z_{min} we finally get

$$z_{min} = i\frac{L}{\pi\xi_N}\sqrt{\frac{\gamma\sqrt{\tilde{\Omega}}}{\gamma_B\sqrt{\tilde{\Omega}}+\coth\left\{\frac{d_F}{\xi_F}\sqrt{\tilde{\Omega}}\right\}}\frac{\xi_N}{d_N}+\Omega}. \quad \text{(B10)}$$

Note that the imaginary parts of the roots of both groups $(z_{k,F}, z_{k,N})$ do not exceed their real parts. It means that inequality (B8) guarantees the smallness of Re z_{min} compared to Re$(z_{k,F}, z_{k,N})$.

Assuming further that the total contribution to I_C from the all the residues at critical points $z_{k\geq 1}$ is small compared to that at $z=z_{min}$,

$$\left|\mathrm{Re}\frac{1}{z_{min}\sinh\pi z_{min}}\right| \gg \Sigma_F + \Sigma_N, \quad \text{(B11)}$$

$$\Sigma_{F(N)} = \left|\mathrm{Re}\sum_k \frac{1}{z_{k,F(N)}\sinh\pi z_{k,F(N)}}\right|, \quad \text{(B12)}$$

we arrive at the following expression for I_C:

$$I_C = \frac{4\pi T}{e}\frac{W}{\gamma_{BN}^2\rho_N}\gamma\,\mathrm{Re}\sum_{\omega>0}^{\infty}\frac{G_0^2\Delta^2k^2(S_F+S_N)}{D^2\omega^2q\xi_N\sinh(qL)},$$

$$S_F = \frac{\xi_F^2}{\xi_N^2}\left[1+\frac{2vd_F}{\xi_F}\sinh^{-1}\frac{2vd_F}{\xi_F}\right]\frac{u^2}{v}\coth\frac{vd_F}{\xi_F},$$

$$S_N = \gamma\left[1+\frac{2ud_N}{\xi_N}\sinh^{-1}\frac{2ud_N}{\xi_N}\right]\frac{v^2}{u}\coth\frac{ud_N}{\xi_N}, \quad \text{(B13)}$$

where $u=\sqrt{\Omega-q^2\xi_N^2}$, $v=\sqrt{\tilde{\Omega}-q^2\xi_F^2}$, and the characteristic wave vector q is given by

$$q = \frac{1}{\xi_N}\sqrt{\frac{\xi_N}{d_N}\frac{\gamma\sqrt{\tilde{\Omega}}}{\gamma_B\sqrt{\tilde{\Omega}}+\coth\left\{\frac{d_F}{\xi_F}\sqrt{\tilde{\Omega}}\right\}}+\Omega}. \quad \text{(B14)}$$

The coefficients k and D in Eq. (B13) have the form

$$k = \frac{1}{u^2}-\frac{\gamma_{BN}}{\gamma_{BF}}\frac{\xi_F}{\xi_N}\frac{1}{v^2},$$

$$D = \left(\frac{d_N}{\xi_N}+\gamma\frac{\xi_F^2}{\xi_N^2}\frac{d_F}{\xi_F}\right)\coth\frac{ud_N}{\xi_N}\coth\frac{vd_F}{\xi_F}$$
$$+\left(\gamma_B v\frac{d_N}{\xi_N}+\frac{\xi_F^2}{\xi_N^2}\frac{\gamma}{v}\right)\coth\frac{ud_N}{\xi_N}+\left(\gamma_B u\frac{d_F}{\xi_F}\frac{\xi_F^2}{\xi_N^2}+\frac{1}{u}\right)\coth\frac{vd_F}{\xi_F}$$
$$+\frac{v}{u}\left(\gamma_B+\gamma\frac{d_N}{\xi_N}\right)+\frac{\xi_F^2}{\xi_N^2}\frac{u}{v}\left(\gamma_B+\frac{d_F}{\xi_F}\right). \quad \text{(B15)}$$

From Eqs. (B8) and (B10) it follows that approximation (B14) for q is valid if

$$\frac{\xi_F^2}{\eta h\xi_N^2} \ll \frac{d_N}{\xi_N} \ll \eta, \quad \text{(B16)}$$

where

$$\eta = \begin{cases}\frac{1}{\gamma}\sqrt{\gamma_B^2+\gamma_B\sqrt{2h^{-1}+h^{-1}}}, & \frac{d_F}{\xi_F}\gg 1/\sqrt{h}\\ \frac{1}{\gamma}\sqrt{\gamma_B^2+2\gamma_B\frac{\xi_F}{d_F}\frac{\Omega}{h^2}+\frac{\xi_F^2}{d_F^2h^2}}, & \frac{d_F}{\xi_F}\ll 1/\sqrt{h},\end{cases} \quad \text{(B17)}$$

where $h=H/\pi T_C\,\mathrm{sgn}\,\omega$. To get Eq. (B16) we additionally restricted ourselves by considering the most interesting from the practical point of view situation when

$$h \gg T/T_C, \quad \xi_F \ll \xi_N. \quad \text{(B18)}$$

It follows from inequalities (B16) and (B17) that the range of validity of expression (B10) is the larger, the smaller is the parameter γ and thickness of F film d_F or the larger is the γ_B. At $\gamma=0$ or $\gamma_B\to\infty$ rigid boundary conditions take place at NF interface and expression (B10) is valid for arbitrary thickness of the normal film.

From Eqs. (B11) and (B12) it follows that in the limit of thin F and N films, $d_F/\xi_F \ll 1/\sqrt{h}$ and $d_N/\xi_N \ll 1/\sqrt{\Omega}$, the result (B13)–(B15) is valid if conditions (B16) are fulfilled. Inequality (B11) provides also the restriction on the thicknesses d_F and d_N of F and N films. Physically, it comes from the fact that with d_F (d_N) increase the full supercurrent flowing across F (N) film is enlarged proportionally to d_F (d_N). Therefore the smallness of this current component compared to contribution to I_C, which is accumulated in vicinity of FN interface, results in

$$d_F\,\mathrm{Re}(q) \ll \exp\left\{\frac{L}{\xi_F}\sqrt{h}\right\}. \quad \text{(B19)}$$

$$d_N\,\mathrm{Re}(q) \ll \exp\left\{L\left(\frac{\sqrt{\Omega}}{\xi_N}-q\right)\right\}. \quad \text{(B20)}$$

Finally we should take into account that the form of the boundary conditions (3) is valid for relatively large γ_{BN}, thus providing additional restriction for application of Eq. (B13), which sets the limit on the distance between superconducting electrodes,

$$L \gg \mathrm{Re}\left(\frac{1}{q}\mathrm{arctanh}\frac{1}{\gamma_{BN}q\xi_N}\right). \quad \text{(B21)}$$

From Eqs. (B14), (B18), and (B21) it follows that inequality (B19) is always fulfilled for experimentally reasonable thickness of F layer and does not apply a serious restriction on the use of Eq. (B13).

Taking into account inequality (B16) we can further simplify the expression for the critical current (B13) and transform it into the formula

$$I_C = \frac{2\pi T}{e}\frac{d_N}{\xi_N}\frac{W}{\gamma_{BN}^2\rho_N}\mathrm{Re}\sum_{\omega>0}^{\infty}\frac{G_0^2\Delta^2}{\omega^2q\xi_N\sinh(qL)}, \quad \text{(B22)}$$

in which the dependence of $I_C(d_F)$ enters only via functional dependence $q(d_F)$ determined by Eq. (B14). It is important to note that to use expression (B22) it is enough to be in the range of parameters, which guarantees the implementation of Eq. (B16).

*janaph@gmail.com

[1] V. V. Ryazanov, V. A. Oboznov, A. Yu. Rusanov, A. V. Veretennikov, A. A. Golubov, and J. Aarts, Phys. Rev. Lett. **86**, 2427 (2001).

[2] S. M. Frolov, D. J. Van Harlingen, V. A. Oboznov, V. V. Bolginov, and V. V. Ryazanov, Phys. Rev. B **70**, 144505 (2004).

[3] S. M. Frolov, D. J. Van Harlingen, V. V. Bolginov, V. A. Oboznov, and V. V. Ryazanov, Phys. Rev. B **74**, 020503(R) (2006).

[4] V. A. Oboznov, V. V. Bol'ginov, A. K. Feofanov, V. V. Ryazanov, and A. I. Buzdin, Phys. Rev. Lett. **96**, 197003 (2006).

[5] T. Kontos, M. Aprili, J. Lesueur, F. Genet, B. Stephanidis, and R. Boursier, Phys. Rev. Lett. **89**, 137007 (2002).

[6] H. Sellier, C. Baraduc, F. Lefloch, and R. Calemczuk, Phys. Rev. B **68**, 054531 (2003).

[7] Y. Blum, A. Tsukernik, M. Karpovski, and A. Palevski, Phys. Rev. B **70**, 214501 (2004).

[8] C. Surgers, T. Hoss, C. Schonenberger, and C. Strunk, J. Magn. Magn. Mater. **240**, 598 (2002).

[9] C. Bell, R. Loloee, G. Burnell, and M. G. Blamire, Phys. Rev. B **71**, 180501(R) (2005).

[10] V. Shelukhin, A. Tsukernik, M. Karpovski, Y. Blum, K. B. Efetov, A. F. Volkov, T. Champel, M. Eschrig, T. Lofwander, G. Schon, and A. Palevski, Phys. Rev. B **73**, 174506 (2006).

[11] M. Weides, K. Tillmann, and H. Kohlstedt, Physica C **437-438**, 349 (2006).

[12] M. Weides, M. Kemmler, H. Kohlstedt, A. Buzdin, E. Goldobin, D. Koelle, and R. Kleiner, Appl. Phys. Lett. **89**, 122511 (2006).

[13] M. Weides, M. Kemmler, E. Goldobin, H. Kohlstedt, R. Waser, D. Koelle, and R. Kleiner, Phys. Rev. Lett. **97**, 247001 (2006).

[14] J. Pfeiffer, M. Kemmler, D. Koelle, R. Kleiner, E. Goldobin, M. Weides, A. K. Feofanov, J. Lisenfeld, and A. V. Ustinov, Phys. Rev. B **77**, 214506 (2008).

[15] H. Sellier, C. Baraduc, F. Lefloch, and R. Calemczuk, Phys. Rev. Lett. **92**, 257005 (2004).

[16] F. Born, M. Siegel, E. K. Hollmann, H. Braak, A. A. Golubov, D. Yu. Gusakova, and M. Yu. Kupriyanov, Phys. Rev. B **74**, 140501(R) (2006).

[17] J. W. A. Robinson, S. Piano, G. Burnell, C. Bell, and M. G. Blamire, Phys. Rev. Lett. **97**, 177003 (2006).

[18] S. Piano, J. W. A. Robinson, G. Burnell, and M. G. Blamire, Eur. Phys. J. B **58**, 123 (2007).

[19] J. W. A. Robinson, S. Piano, G. Burnell, C. Bell, and M. G. Blamire, Phys. Rev. B **76**, 094522 (2007).

[20] M. Yu. Kupriyanov, A. A. Golubov, and M. Siegel, Proc. SPIE **6260**, 227 (2006).

[21] F. S. Bergeret, A. F. Volkov, and K. B. Efetov, Rev. Mod. Phys. **77**, 1321 (2005).

[22] F. S. Bergeret, A. F. Volkov, and K. B. Efetov, Phys. Rev. Lett. **86**, 4096 (2001).

[23] A. Kadigrobov, R. I. Shekhter, and M. Jonson, EPL **54**, 394 (2001).

[24] F. S. Bergeret, A. F. Volkov, and K. B. Efetov, Phys. Rev. B **64**, 134506 (2001).

[25] A. F. Volkov, F. S. Bergeret, and K. B. Efetov, Phys. Rev. Lett. **90**, 117006 (2003).

[26] F. S. Bergeret, A. F. Volkov, and K. B. Efetov, Phys. Rev. B **68**, 064513 (2003).

[27] Z. Pajović, M. Božović, Z. Radović, J. Cayssol, and A. Buzdin, Phys. Rev. B **74**, 184509 (2006).

[28] B. Crouzy, S. Tollis, and D. A. Ivanov, Phys. Rev. B **75**, 054503 (2007).

[29] I. B. Sperstad, J. Linder, and A. Sudbo, Phys. Rev. B **78**, 104509 (2008).

[30] Y. Tanaka and A. A. Golubov, Phys. Rev. Lett. **98**, 037003 (2007); Y. Asano, Y. Sawa, Y. Tanaka, and A. A. Golubov, Phys. Rev. B **76**, 224525 (2007).

[31] M. Eschrig, J. Kopu, J. C. Cuevas, and G. Schon, Phys. Rev. Lett. **90**, 137003 (2003); M. Eschrig and T. Lofwander, Nat. Phys. **4**, 138 (2008).

[32] V. Braude and Yu. V. Nazarov, Phys. Rev. Lett. **98**, 077003 (2007).

[33] M. Houzet and A. I. Buzdin, Phys. Rev. B **76**, 060504(R) (2007).

[34] A. F. Volkov, A. Anishchanka, and K. B. Efetov, Phys. Rev. B **73**, 104412 (2006).

[35] A. F. Volkov, Ya. V. Fominov, and K. B. Efetov, Phys. Rev. B **72**, 184504 (2005).

[36] T. Löfwander, T. Champel, and M. Eschrig, Phys. Rev. B **75**, 014512 (2007).

[37] T. Champel, T. Lofwander, and M. Eschrig, Phys. Rev. Lett. **100**, 077003 (2008).

[38] A. V. Galaktionov, M. S. Kalenkov, and A. D. Zaikin, Phys. Rev. B **77**, 094520 (2008).

[39] F. S. Bergeret, A. F. Volkov, and K. B. Efetov, Appl. Phys. A: Mater. Sci. Process. **89**, 599 (2007).

[40] K. B. Efetov, I. A. Garifullin, A. F. Volkov, and K. Westerholt, Springer Tracts Mod. Phys. **227**, 251 (2008).

[41] R. S. Keizer, S. T. B. Goennenwein, T. M. Klapwijk, G. Miao, G. Xiao, and A. Gupta, Nature (London) **439**, 825 (2006).

[42] I. Sosnin, H. Cho, V. T. Petrashov, and A. F. Volkov, Phys. Rev. Lett. **96**, 157002 (2006).

[43] N. M. Chtchelkatchev and I. S. Burmistrov, Phys. Rev. B **68**, 140501(R) (2003).

[44] I. S. Burmistrov and N. M. Chtchelkatchev, Phys. Rev. B **72**, 144520 (2005).

[45] T. Champel and M. Eschrig, Phys. Rev. B **72**, 054523 (2005).

[46] M. Houzet and A. I. Buzdin, Phys. Rev. B **74**, 214507 (2006).

[47] M. A. Maleki and M. Zareyan, Phys. Rev. B **74**, 144512 (2006).

[48] Y. V. Fominov, A. F. Volkov, and K. B. Efetov, Phys. Rev. B **75**, 104509 (2007).

[49] A. F. Volkov and A. Anishchanka, Phys. Rev. B **71**, 024501 (2005).

[50] A. F. Volkov and K. B. Efetov, Phys. Rev. B **78**, 024519 (2008).

[51] B. Crouzy, S. Tollis, and D. A. Ivanov, Phys. Rev. B **76**, 134502 (2007).

[52] T. Yu. Karminskaya and M. Yu. Kupriyanov, Pis'ma Zh. Eksp. Teor. Fiz. **85**, 343 (2007) [JETP Lett. **85**, 286 (2007)].

[53] T. Yu. Karminskaya and M. Yu. Kupriyanov, Pis'ma Zh. Eksp. Teor. Fiz. **86**, 65 (2007) [JETP Lett. **86**, 61 (2007)].

[54] T. Yu. Karminskaya and M. Yu. Kupriyanov, Pis'ma Zh. Eksp. Teor. Fiz. **87**, 657 (2007) [JETP Lett. **87**, 570 (2008)].

[55] F. S. Bergeret, A. F. Volkov, and K. B. Efetov, Phys. Rev. Lett. **86**, 3140 (2001).

[56] E. A. Koshina and V. N. Krivoruchko, Phys. Rev. B **63**, 224515 (2001); V. N. Krivoruchko and E. A. Koshina, *ibid.* **64**, 172511 (2001).

[57] A. A. Golubov, M. Yu. Kupriyanov, and Ya. V. Fominov, Pis'ma Zh. Eksp. Teor. Fiz. **75**, 223 (2002) [JETP Lett. **75**, 190 (2002)].

[58] A. A. Golubov, M. Yu. Kupriyanov, and Ya. V. Fominov, Pis'ma

Zh. Eksp. Teor. Fiz. **77**, 609 (2003) [JETP Lett. **77**, 510 (2003)].
[59] Ya. M. Blanter and F. W. J. Hekking, Phys. Rev. B **69**, 024525 (2004).
[60] G. Nowak, H. Zabel, and K. Westerholt, Phys. Rev. B **78**, 134520 (2008).
[61] L. Usadel, Phys. Rev. Lett. **25**, 507 (1970).
[62] A. I. Buzdin, Rev. Mod. Phys. **77**, 935 (2005).
[63] M. Yu. Kuprianov and V. F. Lukichev, Zh. Eksp. Teor. Fiz. **94**, 139 (1988) [Sov. Phys. JETP **67**, 1163 (1988)].
[64] J. Bass and W. P. Pratt, Jr., J. Phys.: Condens. Matter **19**, 183201 (2007).
[65] S. M. Frolov, M. J. A. Stoutimore, T. A. Crane, D. J. Van Harlingen, V. A. Oboznov, V. V. Ryazanov, A. Ruosi, C. Granata, and M. Russo, Nat. Phys. **4**, 32 (2008).
[66] V. I. Zdravkov, A. S. Sidorenko, G. Obermeier, S. Gsell, M. Schreck, C. Muller, S. Horn, R. Tidecks, and L. R. Tagirov, Phys. Rev. Lett. **97**, 057004 (2006).
[67] A. S. Sidorenko, V. Zdravkov, J. Kehrle, R. Morari, G. Obermeier, S. Gsell, M. Schreck, C. Muller, V. Ryazanov, S. Horn, L. R. Tagirov, and R. Tidecks, J. Phys.: Conf. Ser. **150**, 052242 (2009).
[68] K. K. Likharev, Rev. Mod. Phys. **51**, 101 (1979).
[69] A. A. Golubov, M. Yu. Kupriyanov, and E. Il'ichev, Rev. Mod. Phys. **76**, 411 (2004).